CHAPTER 1 ENERGY AREA

GLYCEROL ELECTROOXIDATION FOR ENERGY CONVERSION USING METAL NANOPARTICLES

Martin Daniel Trejo Valdez*, Luciana López Escobar, María Elena Manríquez Ramírez, Rodrigo Andrés Espinosa Flores

[1]Instituto Politécnico Nacional, Escuela Superior de Ingeniería Química e Industrias Extractivas (ESIQIE), Laboratorio de Investigación en Nanomateriales y Energías Limpias, Zacatenco, Edificio Z5 P.B., 07300, Ciudad de México.

mtrejov@ipn.mx

Trejo Valdez, M. D., López Escobar, L., Manríquez Ramírez, M. E., & Espinosa Flores, R. A. (2023). Glycerol electrooxidation for energy conversion using metal nanoparticles. In E. San Martín-Martínez (Ed.). *Research advances in nanosciences, micro and nanotechnologies. Volume IV* (pp. 155-176). Barcelona, Spain: Omniascience.

Abstract

Glycerol, also called glycerin, propanetriol or trihydroxypropane, is an alcohol with three -OH groups, which is obtained as a by-product in the production of biodiesel and is currently generated in quantities that exceed demand. In addition, crude glycerol causes significant pollution, as it contains methanol residues, which can be toxic to organisms present in aquifers. Glycerol can be transformed into other value-added products by chemical or enzymatic catalysis. Its transformation by electrochemical route is more attractive since it can be applied to the development of alkaline direct glycerol fuel cells (ADGFC). Transition element metal nanoparticles and some of its metallic oxides are commonly used as electrocatalysts in the anode of ADGFCs due to their high chemical stability and excellent catalytic activity. Therefore, the present work deals with the synthesis of metal nanoparticles of Gold, Platinum, Nickel and their bimetallic combinations to study their electrocatalytic activity in the oxidation of glycerol and to analyze their potential application in the development of ADGFC fuel cells. The electrocatalytic properties of metal nanoparticles were evaluated by using cyclic voltammetry and chronoamperometry coupled to ATR-FTIR spectroscopy (Attenuated Total Reflection- Fourier Transform Infrared Spectroscopy).

Keywords: Metal nanoparticles, alkaline glycerol fuel cells, glycerol oxidation, Chronoamperometry coupled to ATR-FTIR.

1. Introduction

Glycerol ($C_3H_8O_3$) is an alcohol with three hydroxyl groups, at room temperature it has a viscous, colorless appearance, is odorless, hygroscopic, insoluble in hydrocarbons and has a slightly sweet taste, commercially known as Glycerin. It is a pH-neutral substance (does not release hydronium or hydroxyl cations when dissolved in water) and is chemically stable under stable storage and handling conditions [1, 2]. It has a boiling point at 290 °C, at this temperature it decomposes generating Acrolein (a highly toxic compound). Generally, glycerol is used in medical preparations, pharmaceuticals, cosmetics, food additives and various products such as glycolic acid, oxalic acid, acetic acid, formic acid, glyceric acid, dihydroxyacetone, tartronic acid, and hydroxypyruvic acid. Glycerol has had a growing production over the years, since it is a by-product in the manufacture of biodiesel, therefore, due to these large volumes generated, which are greater than those demanded are, it has become an important pollutant of wastewater and aquifers [3, 4].

The development of Alkaline Direct Glycerol Fuel Cells (ADGFCs) is quite attractive given their high energy density whose theoretical value is close to 6.4 kW*h/L, which is advantageous in its application since it also reduces its environmental impact by transforming it into additional value-added products. The main challenge in the commercialization of ADGFC cells lies in the kinetics of the glycerol oxidation reaction, i.e. the breaking of covalent C-C bonds and its complete oxidation to CO_2 [5, 6].

Due to their chemical stability and high catalytic activity, Pt nanoparticles are commonly used in research works dealing with primary anode electrolysis of ADGFCs. However, Pt is a naturally scarce and expensive material and suffers from CO poisoning [7]. Moreover, the technological development leading to the commercialization of Anion Exchange Membrane-Direct Glycerol Fuel Cells (AEM-DGFCs) is slowed down by technical issues such as high platinum group metal loading on the anode electrode, low selectivity and poor long-term stability of the catalyst. In addition, the electrooxidation of glycerol conducted by platinum metal leads to the formation of several by-products, which are associated with multiple reaction steps. For example, several works report the formation of C3 products such as glyceraldehyde, dihydroxyacetone, tartronate, glycerate and mesoxalate; C2 products such as glycolate, glyoxylate and oxalate; and C1 products such as formate and CO_3^{2-} [8 –12]. In this sense, international research

groups focused their works on optimizing the catalyst chemical composition, particle size and morphology, structure and metal-support interaction to achieve excellent electrocatalytic performance of the glycerol oxidation reaction in an alkaline environment [13 – 17]. For instance, an alternative approach is the use of Pt catalysts modified with other metals such as Pd, Cu, Au, Ag and Sn, or by combining with metal oxides such as NiO, CuO, MnO_2 and CeO_2 [18 – 25].

Among the above-mentioned metals, nickel is a low-cost and earth-abundant element, and its crystalline structure and lattice parameters are comparable with those of platinum, thereby allowing the facile formation of well-defined alloyed structures. Thus, in this work we focused on the study of the electrooxidation of glycerol using bimetallic PtNi nanoparticles in alkaline medium. The results obtained with this material are compared with those obtained using gold and platinum nanoparticles. Electrochemical kinetic of glycerol oxidation was evaluated by means of cyclic and linear hydrodynamic voltammetry techniques.

2. Experimental

2.1. *Materials and reagents*

Sodium Borohydride $NaBH_4$ (Fluka Analytical ≥99.0 %, Lot # STBC6399V), Sodium citrate tribasic dehydrate $Na_3C_6H_5O_7 \cdot 2H_2O$ (Sigma-Aldrich ≥99.0 %, Lot # SLBP0031V), Gold (III) Chloride Trihydrate $HAuCl_4 \cdot 3H_2O$ (Sigma-Aldrich ≥99.9 % Lot # MKCJ4933), Potassium Iodide KI (Baker ≥99.0 % Lot # A39C76), Nickel (II) nitrate hexahydrate $Ni(NO_3)_2 \cdot 6H_2O$ (Sigma-Aldrich ≥97.0 % Lot # BCBR5231V), Chloroplatinic acid hexahydrate $H_2PtCl_6 \cdot 6H_2O$ (Sigma-Aldrich ≥99.9 %), Vulcan Carbon Black VXC-72R (Gently furnished by Química Rana S.A. DE C.V. Lot # 4267369, Mizu Técnica), Sílice < 0.5, Isopropilic alcohol (ACS FERMONT, 99.9 % Lot # 039131), Nafión™ 117 containing solution ~5 % in a mixture of lower aliphatic alcohols and water (Sigma-Aldrich Lot # BCCF9827). The chemical reagents were used as received and all solutions were prepared using bidestilled and deionized water.

2.2. *Catalysts preparation*

For the preparation of Pt-Ni nanoparticles supported on carbon, a two-step method was used. In a first step, a volume of 160 μL of 0.1 M $Ni(NO_3)_2$ solution and 260 μL of a platinum standard solution of concentration 0.0025 g/ml were

added to a beaker containing 10 mL of deionized H_2O. This mixture was placed on a magnetic stirring plate and stirred with the aid of a magnetic stir bar. Then, 0.005 g of Vulcan charcoal was added into the solution and stirring was continued until a homogeneous dispersion was obtained. A volume of 250 μL of 0.1 M sodium citrate was then added as surfactant. Finally, a volume of 250 μL of reducing agent sodium borohydride was added. The solution was left to stir for 30 minutes and the resulting dispersion of carbon nanoparticles was poured into test tubes and centrifuged for 20 minutes to separate the supernatant. The material with the NPs was washed repeatedly with absolute ethanol. In a final step the carbon supported metal particles were centrifuged and dispersed in only 1 mL of absolute ethanol. This dispersion was used to prepare an ink that was placed on the surface of a rotating glassy carbon disk electrode for electrocatalytic study of the material. The ink was prepared by mixing 250 uL of the nanoparticles dispersion with 50 μL of Nafion and 150 μL of acetone. The mixture was homogenized in an ultrasonic bath by sonicated for a time of 10 minutes.

In order to compare the electrokinetic performance of Pt-Ni bimetallic particles, Pt and Au metallic nanoparticles were also synthesized. The synthesis of Pt particles supported on Vulcan carbon was performed in a similar manner than PtNi catalyst by adding only the corresponding volume of precursor solution. On the other hand, and like the synthetic route of bimetallic particles, a volume of 250 μL of a 0.01 M $HAuCl_4$ aqueous solution was used for the synthesis of Au nanoparticles.

2.3. *Working electrode preparation*

The surface of a disk carbon glass of 1.2 cm^2 diameter was used as substrate for the electrochemical test. First, the carbon electrode was previously polished with a commercial silica alumina solution (Masterpolish) and after this, the surface was then rinsed with distilled water and with isopropyl alcohol. The dry and clean electrode was weighed on an analytical balance and then coated with 50 μL of the ink containing carbon supported nanoparticles. The solvents of the ink were evaporated, and the electrode was coated a couple of times with the ink. Once the excess of solvents was evaporated the coated electrode was used for electrochemical test.

2.4. *Electrochemical Test and Product Analysis*

Cyclic voltammetry (CV) and Electrochemical Impedance Spectroscopy (EIS) were carried out on an AUTOLAB potentiostat/galvanostat PGSTAT302 N, in

a three-electrode configuration cell using an ink-coated glass carbon electrode as the working electrode, a platinum wire as the counter electrode, and a Silver/Silver Chloride (Ag/AgCl) as the reference electrode in a 0.1 M KOH aqueous electrolyte. For Cyclic Voltammetry (CV): scans were performed in the potential range from -0.7 to + 0.5 V vs SHE.

Chronoamperometry coupled to ATR-FTIR spectroscopy was used to analyze glycerol oxidation products. This test was carried out on an AUTOLAB potentiostat/galvanostat PGSTAT302 N but with a different cell arrangement. A custom-made three electrode cell that fitted on top of the ATR crystal was machined from polytetrafluoroethylene (PTFE) fitted with a glassy carbon rod as counter electrodes and quasi-reference. The working electrode was a 3 mm diameter graphite electrode (GE). Since inorganic nitrate ions provide a broad and intense IR band near 1400 cm^{-1}, resulting from out-of-phase stretching for nitrate-containing compounds, for these spectro electrochemical tests the electrolyte was 0.1 M KOH electrolyte, since the spectrum obtained will not have interfering bands. It is indeed worth mentioning that a background was subtracted before collecting the ATR-FTIR scans. An aqueous solution containing 0.1 M KOH electrolyte was degassed beforehand under sonication for 20 min, and then N_2 was bubbled into the electrolyte for 20 minutes to purge O_2. This N_2-saturated solution was transferred to the custom-made PTFE three-electrode cell and a background spectrum was collected at this point.

2.5. *Structural samples characterization*

The morphology of the samples was observed using a transmission electron microscopy (JEM-ARM200CF) which was operated in TEM or STEM mode with acceleration voltages of 80–200 kV. It was installed with a cold electron gun cathode and spherical aberration corrector for the STEM mode. The microscope had coupled detectors for surface chemical analysis of the selected area by X-ray.

3. Results and discussion

3.1. *Electrocatalytic activity of gold nanoparticles (Au-NPs)*

The Au-NPs were applied as a conductive ink on a glassy carbon disk electrode as described in the experimental part and adapted as a working electrode in a three-electrode electrolytic cell. An Ag/AgCl electrode was used as reference and

a platinum wire as auxiliary electrode. 0.1 M KOH solution was placed in the cell as the supporting electrolyte and saturated with nitrogen gas to displace dissolved oxygen. After purging with N_2 gas, a voltammogram was plotted starting from an initial potential (Ei) of -698 mV to an intermediate potential (E_1) of +500 mV (anodic sweep) from which the direction of the applied potential was reversed in the cathodic direction to a final potential value (E_f) identical to E_i. In Figure 1 were shown the different voltammograms obtained from the scans varying, for each test, the potential sweep rates from 5 to 20 mV/s. This figure also shows the voltammogram obtained from the support electrolyte (KOH 0.1M) in which the evolution of the anodic capacitive current in the range -0.698 to +0.5 V is observed. For this anodic zone it is deduced that, when increasing the potential, only a slight oxidation of the nanoparticles appears at 0.5 V which determines the anodic limit of the working electrode. However, when the direction of the applied potential is changed to cathodic scanning, a reduction wave between -0.2 and -0.5 V is observed, which is related to the reduction of surface gold ions in the metallic nanoparticles.

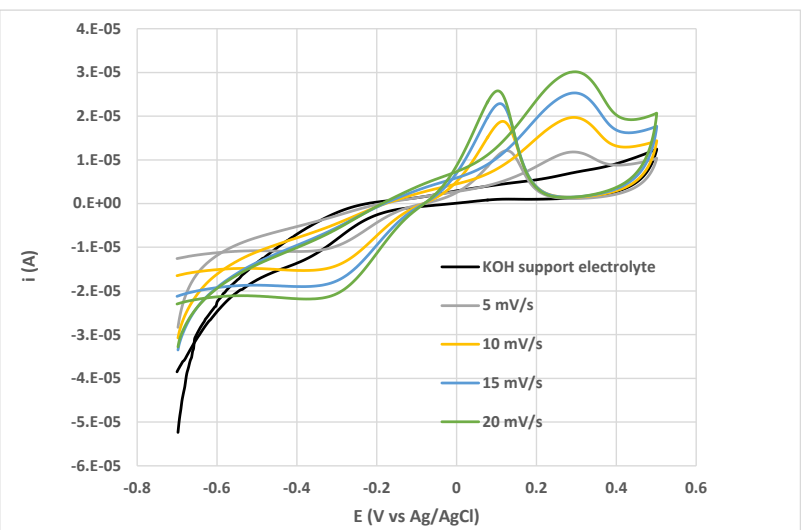

Figure 1. Cyclic Voltammograms obtained from the analysis of glycerol catalyzed by Au NPs. Measurement conditions: 0.1M KOH, Ei=-0.698 V, E1=+ 0.5 V, Ef=-0.698 V, [Glycerol]=2.4 mM.

Once the glycerol is added to the supporting electrolyte, Figure 1 shown that between Ei and -0.2 V a shift of the glycerol measurement currents with respect to the target occurs. This is caused by a capacitive current which is not associated with the electrochemical reaction itself, but with the formation of an electrical double layer on the electrode surface. For voltammograms with glycerol, in the

anodic zone a peak appears at 0.35 V indicating that its oxidation is taking place as an electroactive species, while, when the potential sweep is reversed at 0.1 V, a very pronounced peak appears corresponding to the decomposition of the product formed on the electrode surface.

Cyclic voltammetry was used to explore the ranges of sweep speed and working potential intervals in which oxidation or reduction of the gold nanoparticles does not occur. Moreover, with this technique is seen that the system behaves irreversibly since the ratio between its anodic and cathodic peak intensities is different from the unit. Furthermore, it was evidenced that the glycerol oxidation product formed decomposes when trying to reduce it by reversing the sweep potential direction. Electrode mechanisms are commonly described by using the Testa and Reinmuth notation [26], where letter E is used to denote a heterogeneous electron transfer step, and the letter C to indicate a homogeneous chemical step. In some cases, an electron transfers yields a product that is unstable, and this should be involved in a homogeneous irreversible reaction yielding an electrochemically inactive product:

$$A + e^- \rightleftarrows B \qquad (1)$$

$$B \rightarrow C \qquad (2)$$

Such a case is defined as an EC reaction and its electrochemical analysis is characterized by voltammograms such as those shown by glycerol electrooxidation using the carbon supported Au-Nps.

The results obtained with cyclic voltammetry indicate that it is possible to follow only the glycerol oxidation process. Then, for this process, the electrodynamic kinetic parameters such as the diffusion coefficient and the number of electrons transferred can be determined by using the Randles-Sevcik equation [27]:

$$I_p = 0.496\sqrt{\alpha}\, nFA[G]_{bulk}\sqrt{\frac{FDv}{RT}} \qquad (3)$$

Where:

I_p = peak current intensity [A]

F = Faraday constant [96485.33 C/mol]

n = number of transferred electrons

A=Electrode surface area [cm^2]

D = Diffusion coefficient of the electroactive species [cm^2s^{-1}]

$[G]_{bulk}$= Bulk concentration of electroactive species [$mo^l\ cm^{-3}$]

v = sweep speed [Vs^{-1}]

α = Transfer coefficient (~0.5)

The linear voltammetry technique using a rotating disk electrode (RDE) provides the means to vary the concentration profile at the electrode, since the faster the rotation, the thinner the diffusion layer becomes and the greater the transport-limited flux. The Levich equation models the diffusion and flow conditions of the solution around a rotating disk electrode (RDE), which is characterized by the dependence on the rotational velocity $\varpi^{0.5}$ according to the Eq.4 [26]:

$$I_{lim} = 0.62nFAD^{\frac{2}{3}} \rho^{-\frac{1}{6}} \varpi^{\frac{1}{2}} [G]_{bulk} \ldots\ldots\ldots (4)$$

Where:

I_{lim} = limit current intensity [A]

A = electrode surface area [cm^2]

ρ = dissolvent kinematic viscosity $\left[\frac{cm^2}{s}\right]$

ω = electrode angular rotational speed $\left[\frac{rad}{s}\right]$

and the rest of the constants that have already been defined.

The sweep speed parameter is fixed at 5 mV/s for measurements using the RDE voltammetry and by varying the concentration of glycerol in the cell. The results are shown in Figure 2a where it is observed that the diffusion limit current increases with the addition of glycerol in the electrolytic cell. As is shown in Figure 2b, an absolute standard calibration curve was plotted by taking values in each curve where the limit current is minimum. From this plot, it is concluded that the maximum concentration of glycerol that can be used for working linear hydrodynamic voltammetry is up to 0.7 mol/cm^3. Then, a concentration of 0.662 mol/cm^3 of glycerol is chosen for the hydrodynamic voltammetry experiments but now varying the angular velocity ϖ (see the Figure 3a). According to Levich's postulate, the limiting current densities, j (mA/cm^2*g) should be plotted

as a function of the root of the angular velocity in rad/s, as shown in Figure 3b. Calculating the linear regression of the points in Figure 5 gives a correlation coefficient of 0.9934, which leads to the conclusion that the system behaves linearly according to Levich's equation. By using the eq. 4, the slope of Figure 3b is consistent with n =2 and D=5.75x10^{-6} cm^2/s

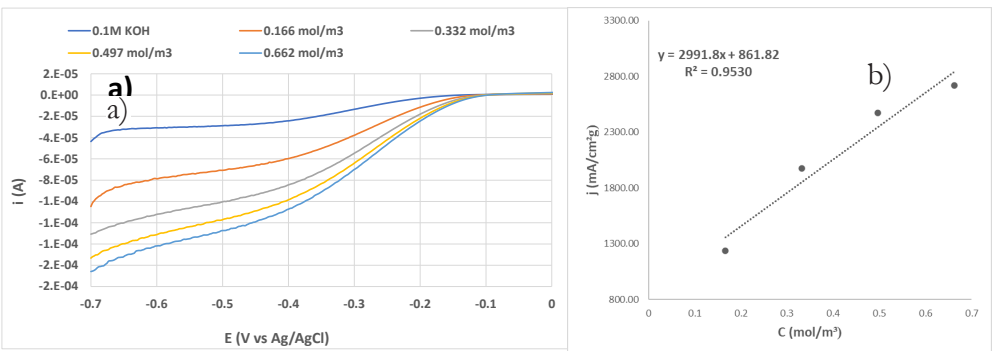

Figure 2. a) RDE Voltammograms obtained by varying the concentration of glycerol and catalyzed by using Au NPs. Measurement conditions: E_i=-0.7 V, Ef=0 V, ω=1500 rpm, υ=0.005 V/s. b) Glycerol calibration curve obtained from the limiting diffusion current values of RDE voltammograms.

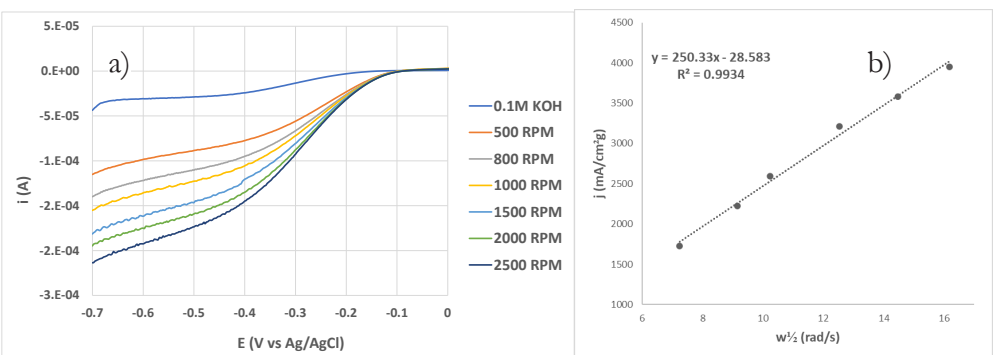

Figure 3. a) RDE Voltammograms obtained by varying the rotational speed of the electrode and catalyzed by using Au-NPs. Measurement conditions: E_i=-0.7 V, Ef=0 V, υ=0.005 V/s, [Glycerol]=6.62 mM. b) The Levich curve obtained from the current limit values.

3.2. *Electrocatalytic activity of platinum nanoparticles (Pt-NPs)*

For this study, the conductive ink applied to the glassy carbon electrode contained Platinum nanoparticles, with which the cyclic voltammograms of Figure 4 were obtained. For each test, the potential sweep rates were increased for a range from 5 to 20 mV/s. The voltammogram of the supporting electrolyte (0.1M

KOH) from a potential value (E_i)=-698 mV to potential (E_1)=+500 mV is seen flat, without any curvature since there is no oxidation or reduction alteration in the material in that potential range. On the other hand, in the measurements with glycerol we observe that the electro-oxidation takes place in a range of -0.1 to -0.2 V when the anodic sweep is being carried out, which is a lower voltage compared to the NP's-Au. The big difference between the first and subsequent sweeps is that from a sweep speed value of 10 mV/s a second oxidation peak is seen at a voltage of -0.2 V, which is evidence that a step transfer of electrons from the glycerol takes place, which is not observed in the case of electrodes modified with the Au-NPs. When the sweep changes to cathodic direction and the applied potential approaches to -0.3 V, only one cathodic peak is observed, which results from an irreversible mechanism. It is evident that the mechanism of glycerol oxidation catalyzed by supported Pt particles is not a simple EC mechanism. As will be discussed later, this electrocatalysis process involves the formation of more than two products.

A 0.662 mM concentration of glycerol is also chosen for the linear hydrodynamic voltammetry experiments by varying the angular velocity. As shown in Figure 5a, the increase of the diffusion current limit is observed with the increase of the angular velocity of the electrode given a correlation coefficient of 0.9933. The slope of plot shown in Figure 5b is consistent with n=6 and $D=6.95x10^{-6}$ cm^2/s.

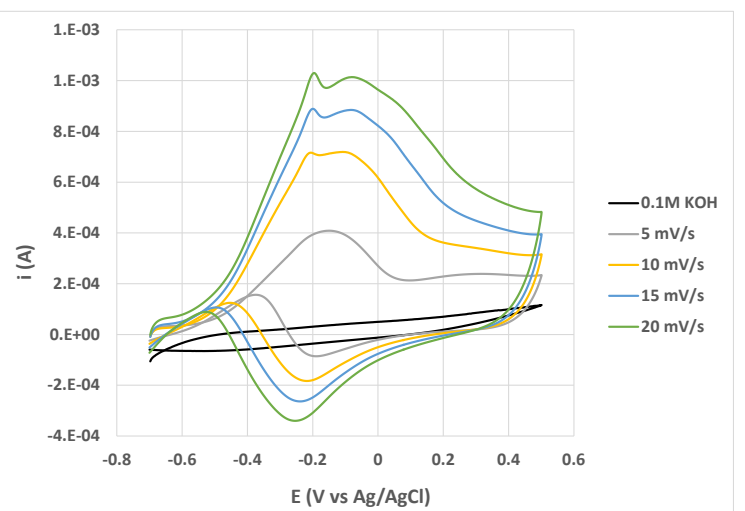

Figure 4. Cyclic voltammograms obtained from the electrocatalysis of glycerol using the Pt-NPs. Measurement conditions: E_i=-0.698 V, E_1=+0.5 V, E_f=-0.698 V, [Glycerol]=2.4 mM.

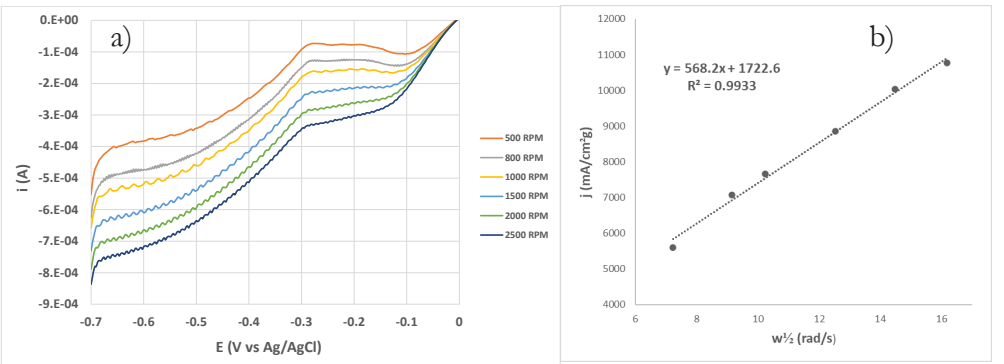

Figure 5. a) RDE Voltammograms obtained by varying the rotational speed of the electrode and catalyzed by using the Pt NPs. Measurement conditions: E_i = -0.7 V, E_f = 0 V, υ =0.005 V/s, [Glicerol] = 6.62mM. b) The Levich curve obtained from the current limit values.

3.3. *Electrocatalytic activity of platinum-nickel nanoparticles (PtNi-NPs)*

In the voltammogram obtained from the supporting electrolyte (see the Figure 6) the evolution of the anodic capacitive current from a potential of -698 mV to 698 mV shows slight oxidation of the bimetallic nanoparticles. However, when the direction of the potential changes to a cathodic sweep, unlike the Pt NP's, a significant reduction of one of the elements composing the PtNi nanoparticles is seen at a potential range of -0.2 to -0.5 V. As soon as glycerol was added to the electrolysis cell and the scanning starts, an anodic peak at -0.18 V

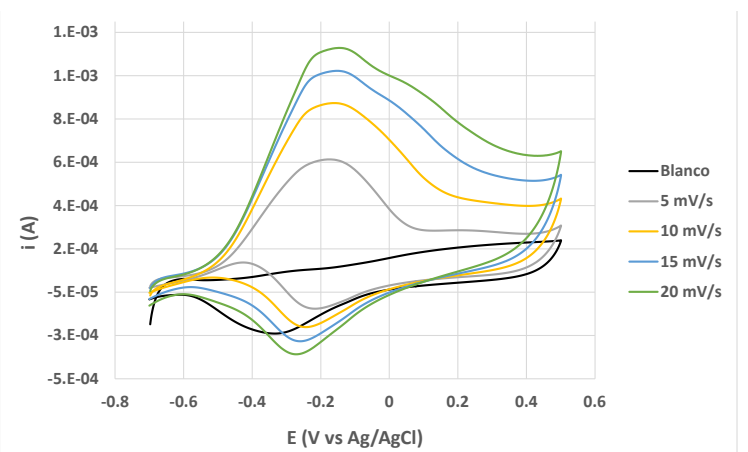

Figure 6. Cyclic Voltammograms obtained from the analysis of glycerol catalyzed by using the Pt-Ni NPs. Measurement conditions: 0.1M KOH, Ei=-0.698 V, E1=+ 0.5 V, Ef=-0.698 V, [Glycerol]=2.4 mM.

is observed, indicating that the oxidation of glycerol as an electroactive specie is taking place. At the highest sweep speed of 20 mV/s, a slight curvature is evident in the anodic zone at approximately 0.1 V, which it can be assumed as an additional oxidation peak, which can involve a second reaction mechanism. Also, when applied potential is inverted to cathodic direction none cathodic signals of glycerol products were observed in voltammogram which is associated with an irreversible chemical mechanism.

As shown in Figure 7a, the increase of the diffusion current limit is observed with the increase of the angular velocity of the electrode given a correlation coefficient of 0.995. The slope of Figure 7b is consistent with n=2 and D=1.75x10^{-7} cm^2/s.

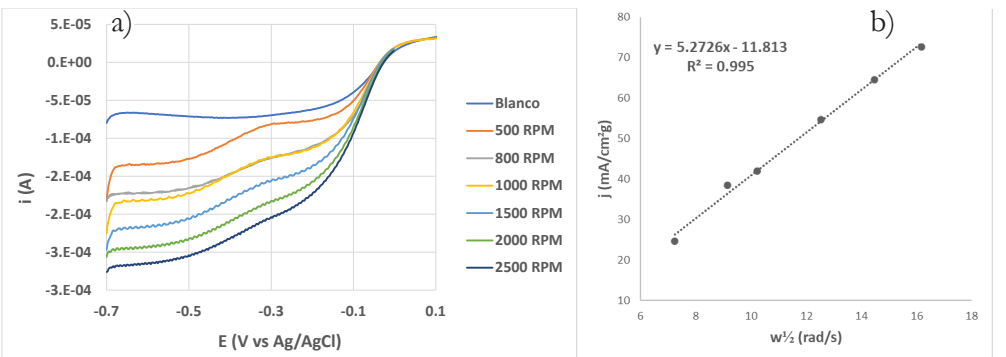

Figure 7. a) Cyclic voltammograms obtained by varying the rotational speed of the electrode and catalyzed by using the Pt-Ni NPs. Measurement conditions: Ei = -0.7 V, Ef = 0 V, υ = 0.005 V/s, [Glicerol] = 6.62 mM. b) The Levich curve obtained from the current limit values.

3.4. *Comparison of Glycerol electro-oxidation kinetics*

The glycerol oxidation process using the different synthesized metal nanoparticles materials (Au, Pt, and PtNi) is shown in the Figure 8. In this figure, the peak current density values were taken from voltammograms of Figures 1, 6 and 7 were plotted against the sweep speed $\nu^{1/2}$ (mV/s). The slope of this plot is related to the standard electrochemical rate constant by means of the dimensionless parameter proposed by Matsuda and Ayabe [28]:

$$\Lambda\sqrt{\frac{FD}{RT}}\,\upsilon^{\frac{1}{2}} = k^{0} \quad (5)$$

From the Figure 8 is appreciated that Pt-Nps shown the highest slope and hence the highest kinetic reaction constant. In addition, as is shown in table 1,

the highest diffusion coefficient of glycerol is obtained by using platinum nanoparticles supported on carbon.

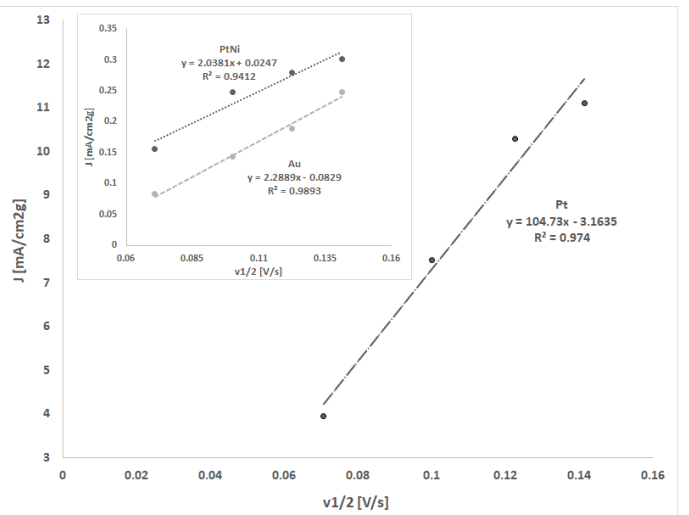

Figure 8. Forward peak current (i_p)versus scan rate for the glycerol oxidation by using the Pt-Nps. The insert corresponds to results obtained by using the Au-Np and PtNi-Nps.

Table 1. Electrochemical parameters of glycerol electrooxidation using the metal nanoparticles.

Metal nanoparticle	n (e-)	D [cm^2s^{-1}]
Au-NPs	2	$3.8296x10^{-7}$
Pt-NPs	6	$4.4852x10^{-7}$
PtNi-NPs	2	$4.48x10^{-7}$

The values of glycerol diffusion coefficient shown in Table 1 are within the range of those reported by D'Errico and co-workers in ref. [29] that were measured by using the Taylor dispersion and Gouy interferometric techniques.

3.5. *Infrared/ATR spectro-electrochemical characterization*

The goal of synthesizing bimetallic NPs with Nickel was due to the possibility of making cheaper catalysts and with less amount of precious metals such as Platinum. Although the electrocatalytic performance of NiPt bimetallic particles followed a very similar pattern to that shown by platinum particles, the electrocatalytic kinetics of the latter turns out to be far superior to that of the former material. Therefore, in this section we focus on the structural characterization of the reaction products on the electrode surface using platinum nanoparticles.

For the identification of the products, infrared spectroscopy tests were performed on the molecules resulting from the anodic reaction of Glycerol with Platinum NPs. Thus, every 5 minutes a spectrum of the oxidized solution was taken for comparison with the initial spectrum at zero time. As can be seen in Figure 9, in the first spectrum is appreciated the signal of the unreacted glycerol solution (t=0), and as the oxidation progresses is shown how progressively a peak appears at a wave number of 1654 cm^{-1}, which is attributed to the formation of a carbonyl group (C=O tension). On the other hand, we also observe the broadening of a tension signal representative of the -OH group from 3654 to 3123 cm^{-1} due to the formation of hydrogen bridges. In addition, we can notice another characteristic absorption band of C-O stress vibrations at 1315 cm^{-1}.

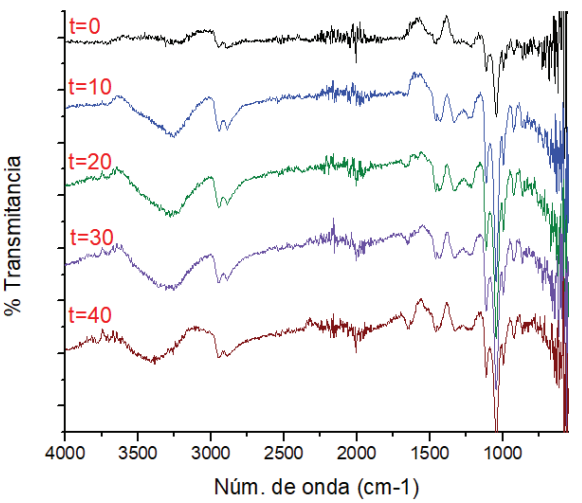

Figure 9. ATR-FTIR spectra of glycerol reduction reaction by using Pt-Nps +0.2 V vs. Ag/AgCl. The acquisition time in minutes was indicated in each spectrum.

From this spectra analysis, and by using a transfer of 6 electrons with the platinum nanoparticles; it is deduced that the glycerol did not only form an aldehyde, but the produced specie was full oxidized to form a carboxylic acid. The proposed electrooxidation mechanism can be similar as that proposed by Coutanceau et. al. [30] which is depicted in the Figure 10. In the initial step, the glycerol in solution travels toward the solution and comes in contact with the electrode surface. Once the glycerol arrives to electrode surface, the oxidation of the primary alcohol by transferring first 2 electrons to form glyceraldehyde. In a second step, this aldehyde formed at the electrode-solution interface is oxidized to glyceric acid via a second transfer of another two electrons. Finally, the Tartronic acid was formed by the oxidation of the glyceric acid via a third transfer of two electrons.

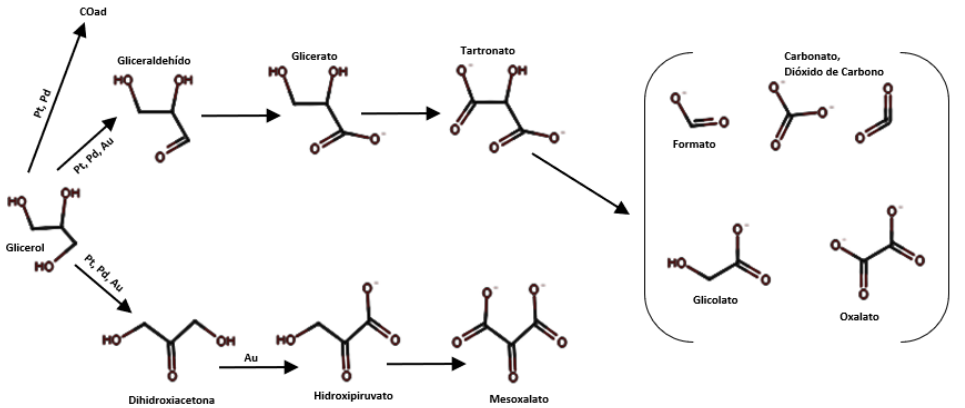

Figure 10. The reaction pathways proposed by Coutanceau *et al.* [30] for electro-oxidation of glycerol on Pt.

3.6. *TEM nanoparticles characterization*

The images obtained by Transmission Electron Microscopy and the analysis performed in the Digital Micrograph Software to measure the interplanar

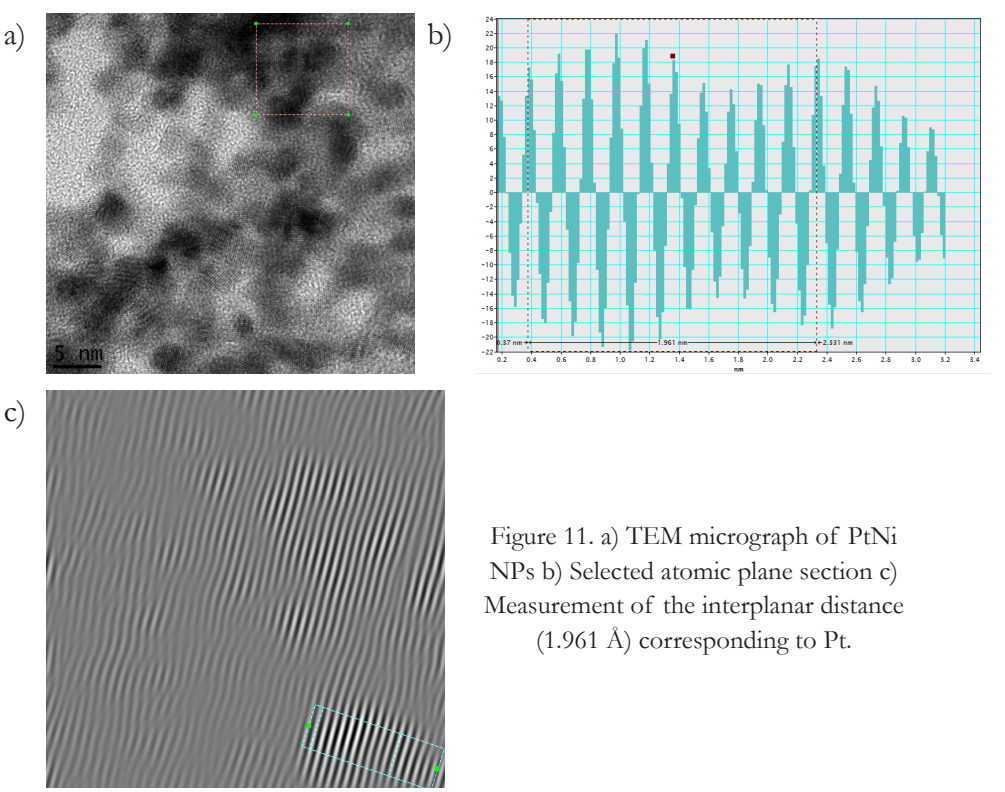

Figure 11. a) TEM micrograph of PtNi NPs b) Selected atomic plane section c) Measurement of the interplanar distance (1.961 Å) corresponding to Pt.

distances of the Platinum nanoparticles are shown in Figures 11. The Figure 11c) show interplanar distances of 1.961 and 2.244 Å, which according to the crystallographic chart of Platinum, correspond to 2θ of 46.2° and 39.76, with which we obtain the diffraction planes of (200) and (111) of Pt respectively.

4. Conclusions

The electrochemical activity of nanoparticles of three metallic nanoparticles (Pt, Au and PtNi) in the electro-oxidation of glycerol was studied to determine which of these materials was the best catalyst for this purpose. The synthesis of such NPs was carried out by a simple chemical method where the precursor solutions of each metal were reduced in situ on to vulcan carbon substrate. The characterization by electroanalytical techniques such as Cyclic Voltammetry and Hydrodynamic Voltammetry (RDE) allowed to visualize the behavior of the NPs in a potential range from -0.7 to 0.7 V(vs Ag/AgCl). It was obtained that all materials shown an irreversible electrode kinetics reaction giving the decomposition of the as formed oxidation product of Glycerol. The diffusion coefficients of glycerol were estimated by hydrodynamic voltammetry whose graphical analysis fitted well to Levich's model, obtaining a number of exchanged electrons of 2 for Au particles, 6 for Pt and 2 electrons by using PtNi bimetallic particles. The reaction mechanism for the electrooxidation of Glycerol was proposed from results obtained by using Pt-NPs and ATR spectroscopy coupled to chronoamperometric analysis. It was deduced that the product formed is a carboxylic acid, which could be tartronic acid.

Acknowledgment and Funding

The authors acknowledge the financial support for developing this work from the Instituto Politécnico Nacional (IPN) through the projects: SIP2241, SIP20230209, and EDI grants. We are grateful for the technical support of the IPN's Centro de Nanociencias y Micro y Nanotecnologías (CNMN).

References

1. Yang, F., Hanna, M. A., & Sun, R. (2012). Value-added uses for crude glycerol–a byproduct of biodiesel production. *Biotechnology for Biofuels* 5, 13. https://doi.org/10.1186/1754-6834-5-13

2. Veljković, V. B., Biberdžić, M. O., Banković-Ilić, I. B., Djalović, I. G., Tasić, M. B., Nježić, Z. B., *et al.* (2018). Biodiesel production from corn oil: a review. *Renewable Sustainable Energy Reviews*, 91, 531-548. https://doi.org/10.1016/j.rser.2018.04.024

3. Tan, H. W., Abdul Aziz, A. R., & Aroua, M. K. (2013). Glycerol production and its applications as a raw material: A review. *Renewable and Sustainable Energy Reviews*, 27, 118-127. https://doi.org/10.1016/j.rser.2013.06.035

4. Md. Rahim, S. A. N., Lee, C. S., Abnisa, F., Aroua, M. K., Daud, W. A. W., Cognet, P. *et al.* (2020). A Review of Recent Developments on Kinetics Parameters for Glycerol Electrochemical Conversion – A by-product of Biodiesel. *Science of the Total Environment*, 705, Article 135137. https://doi.org/10.1016/j.scitotenv.2019.135137

5. Yahya, N., Kamarudin, S. K., Karim, N. A., Masdar, M. S., Loh, K. S., & Lim, K. L. (2019). Durability and performance of direct glycerol fuel cell with palladium-aurum/vapor grown carbon nanofiber support. *Energy Conversion and Management*, 188, 120-130. https://doi.org/10.1016/j.enconman.2019.02.087

6. Geraldes, A. N., Da Silva, D. F., Silva, L. G. A., Spinacé, E. V., Neto, A. O., Dos Santos, M. C. (2015). Binary and ternary palladium based electrocatalysts for alkaline direct glycerol fuel cell. *Journal of Power Sources*, 293, 823-830. https://doi.org/10.1016/j.enconman.2019.02.087

7. Kim, M., Lee, C., Ko, S. M., & Nam, J. M. (2019). Metal alloy hybrid nanoparticles with enhanced catalytic activities in fuel cell applications. *Journal of Solid State Chemistry*, 270, 295-303. https://doi.org/10.1016/j.jssc.2018.11.014

8. Huang, L., Sun, J.-Y., Cao, S.-H., Zhan, M., Ni, Z.-R., Sun, H.-J. *et al.* (2016). Combined EC-NMR and In Situ FTIR Spectroscopic Studies of Glycerol Electrooxidation on Pt/C, PtRu/C, and PtRh/C. *ACS Catalysis*, 6(11), 7686-7695. https://doi.org/10.1021/acscatal.6b02097

9. Velazquez-Hernández, I., Oropeza-Guzmán, M. T., Guerra-Balcázar, M., Alvarez-Contreras, L., & Arjona, N. (2018). Electrocatalytic Promotion of Pt Nanoparticles by Incorporation of Ni(OH)2 for Glycerol Electro-Oxidation: Analysis of Activity and Reaction Pathway. *ChemNanoMat*, 5(1), 68-78. https://doi.org/10.1002/cnma.201800317

10. Wang, C.-Y., Yu, Z.-Y., Li, G., Song, Q.-T., Li, G., Luo, C.-X. *et al.* (2019). Intermetallic PtBi Nanoplates with High Catalytic Activity towards Electro-oxidation of Formic Acid and Glycerol, *ChemElectroChem*, 7(1), 239-245. https://doi.org/10.1002/celc.201901818

11. Kwon, Y., & Koper, M. T. M. (2010). Combining Voltammetry with HPLC: Application to Electro-Oxidation of Glycerol. *Analytical Chemistry*, 82(13), 5420-5424. https://doi.org/10.1002/celc.201901818

12. Martins, C. A., Giz, M. J., & Camara, G. A. (2011). Generation of carbon dioxide from glycerol: Evidences of massive production on polycrystalline platinum. *Electrochimica Acta*, 56(12), 4549-4553. https://doi.org/10.1002/celc.201901818

13. Wang, W., Jing, W., Wang, F., Liu, S., Liu, X., & Lei, Z. (2018). Amorphous ultra-dispersed Pt clusters supported on nitrogen functionalized carbon: A superior electrocatalyst for glycerol electrooxidation. *Journal of Power Sources*, 399, 357-362. https://doi.org/10.1016/j.jpowsour.2018.07.120

14. Zhang, Y., Gao, F., Song, P., Wang, J., Song, T., Wang, C. *et al.* (2019). Superior liquid fuel oxidation electrocatalysis enabled by novel bimetallic PtNi nanorods. *Journal of Power Sources*, 425, 179-185. https://doi.org/10.1016/j.jpowsour.2019.04.001

15. Wu, F., Zhang, L., Lai, J., Niu, W., Luque, R., & Xu, G. (2019). PtCu-O Highly Excavated Octahedral Nanostructures Built with Nanodendrites for Superior Alcohol Electroxidation. *Journal of Materials Chemistry A.*, 14, 8568-8572. https://doi.org/10.1039/C9TA01236B

16. Zhou, Y., Shen, Y., & Xi, J. (2019). Seed-mediated synthesis of PtxAuy@Ag electrocatalysts for the selective oxidation of glycerol. *Applied Catalysis B: Environmental*, 245, 604-612. https://doi.org/10.1016/j.apcatb.2019.01.009

17. Sieben, J. M., Alvarez, A. E., & Sanchez, M. D. (2023). Glycerol electrooxidation on carbon-supported Pt-CuO and PtCu-CuO catalysts. *Electrochimica Acta*, 439, 141672. https://doi.org/10.1016/j.electacta.2022.141672

18. Lv, H., Sun, L., Xu, D., Suib, S., & Liu, B. (2019). One-pot aqueous synthesis of ultrathin trimetallic PdPtCu nanosheets for the electrooxidation of alcohols. *Green Chemistry*, 9, 2367-2374. https://doi.org/10.1039/C9GC00741E

19. Castagna, R. M., Sieben, J. M., Alvarez, A. E., & Duarte, M. M. E. (2019). Electrooxidation of ethanol and glycerol on carbon supported PtCu nanoparticles. *International Journal of Hydrogen Energy*, 44(12), 5970-5982. https://doi.org/10.1016/j.ijhydene.2019.01.090

20. Dai, C., Sun, L., Liao, H., Khezri, B., Webster, R. D., Fisher, A. C. *et al.* (2017). Electrochemical production of lactic acid from glycerol oxidation catalyzed by AuPt nanoparticles. *Journal of Catalysis*, 356, 14-21. https://doi.org/10.1016/j.jcat.2017.10.010

21. Garcia, A. C., Ferreira, E. B., Silva de Barros, V. V., Linares, J. J., & Tremiliosi-Filho, G. (2017). PtAg/MnOx/C as a promising electrocatalyst for glycerol electro-oxidation in alkaline medium. *Journal of Electroanalytical Chemistry*, 793, 188-196. https://doi.org/10.1016/j.jelechem.2016.11.053

22. Li, Z., Qiu, G., Jiang, Z., Zhuang, W., Wu, J. & Du, X. (2018). Tuning concave Pt-Sn nanocubes for efficient ethylene glycol and glycerol electrocatalysis. *International Journal of Hydrogen Energy*, 43(50), 22538-22547. https://doi.org/10.1016/j.ijhydene.2018.10.132

23. Sieben, J. M., Alvarez, A. E., & Sanchez, M. D. (2022). Platinum nanoparticles deposited on Cudoped NiO/C hybrid supports as high-performance catalysts for ethanol and glycerol electrooxidation in alkaline medium. *Journal of Alloys and Compounds*, 921, 166112. https://doi.org/10.1016/j.jallcom.2022.166112

24. Li, Z.-.Y., Zhou, J., Tang, L.-S., Fu, X.-P., Wei, H., Xue, M. (2018). Hydroxyl-rich Ceria Hydrate Nanoparticles Enhancing the Alcohol Electrooxidation Performance of Pt catalysts. *Journal of Materials Chemistry A*, 6(5), 2318-2326. https://doi.org/10.1039/C7TA09071D

25. Velázquez-Hernández, I., Zamudio, E., Rodríguez-Valadez, F. J., García-Gómez, N. A., Álvarez-Contreras, L., Guerra-Balcázar, M. *et al.* (2020). Electrochemical valorization of crude glycerol in alkaline medium for energy conversion using Pd, Au and PdAu nanomaterials. *Fuel*, 262, 116556. https://doi.org/10.1016/j.fuel.2019.116556

26. Richard G. Compton, R. G., & Banks, C. E. (2018). *Understanding voltammetry*. (3rd Ed.). New Jersey: World Scientific. https://doi.org/10.1142/q0155

27. Bard, A. J.; & Faulkner, L. R. (2004). *Electrochemical methods: Fundamentals and applications*. Wiley India Pvt. Ltd. Chpt. 6.

28. Matsuda, H., & Ayabe, Y. (1955). Zur Theorie der Randles-Sevčikschen Kathodenstrahl-Polarographie. *Zeitschrift fuer Elektrochmie and Angewandte Physikalische Chemie*, 59(6), 494-503. https://doi.org/10.1002/bbpc.19550590605

29. D'Errico, G., Ortona, O., Capuano, F., & Vitagliano, V. (2004). Diffusion Coefficients for the Binary System Glycerol + Water at 25 °C. A Velocity Correlation Study. *Journal of Chemical & Engineering Data*, 49(6), 1665-1670. https://doi.org/10.1021/je049917u

30. Coutanceau C., Baranton, S., & Bitty Kouamé, R. S. (2019). Selective Electrooxidation of Glycerol into Value-Added Chemical: A Short Overview. *Frontiers in Chemistry*, 7, article 100. https://doi.org/10.3389/fchem.2019.00100